INTECH
open science | open minds

OPEN ACCESS
ARTICLE

International Journal of Advanced Robotic Systems

Safety Supervisory Strategy for an Upper-Limb Rehabilitation Robot Based on Impedance Control

Regular Paper

Lizheng Pan[1], Aiguo Song[1,*], Guozheng Xu[2], Huijun Li[1], Hong Zeng[1] and Baoguo Xu[1]

1 School of Instrument Science and Engineering, Southeast University, Nanjing, China
2 College of Automation, Nanjing University of Posts and Telecommunications, Nanjing, China
* Corresponding author E-mail: a.g.song@seu.edu.cn

Received 25 Dec 2011; Accepted 5 Nov 2012

DOI: 10.5772/55094

Abstract User security is an important consideration for robots that interact with humans, especially for upper-limb rehabilitation robots, during the use of which stroke patients are often more susceptible to injury. In this paper, a novel safety supervisory control method incorporating fuzzy logic is proposed so as to guarantee the impaired limb's safety should an emergency situation occur and the robustness of the upper-limb rehabilitation robot control system. Firstly, a safety supervisory fuzzy controller (SSFC) was designed based on the impaired-limb's real-time physical state by extracting and recognizing the impaired-limb's tracking movement features. Then, the proposed SSFC was used to automatically regulate the desired force either to account for reasonable disturbance resulting from pose or position changes or to respond in adequate time to an emergency based on an evaluation of the impaired-limb's physical condition. Finally, a position-based impedance controller was implemented to achieve compliance between the robotic end-effector and the impaired limb during the robot-assisted rehabilitation training. The experimental results show the effectiveness and potential of the proposed method for achieving safety and robustness for the rehabilitation robot.

Keywords Rehabilitation Robot, Safety and Robustness, Fuzzy Logic, Impedance Control

1. Introduction

Neurologic injuries such as strokes and spinal cord injuries (SCI) cause dysfunction to the neural system and motor function, which generally results in upper-limb impairment and motion disabilities [1, 2, 3]. Conventionally, manual physical therapy is used to help patients with upper-limb impairments regain functional mobility [4]. In the last few years, there has been an increasing interest in using robotic devices to provide rehabilitation therapy for neurologic injuries [5, 6] and most of the paradigms that have been explored have been concerning physical interaction during movement training [7, 8]. Due to the particular conditions of the participants, safety and robustness are strongly addressed in controller design, which has been a critical issue for the rehabilitation robot.

In recent decades, many researchers have done a lot of work on safety in hardware and software designs [9]. For

emergency situations, an emergency-stop button and some specialized mechanical structures have been designed. D.E. Barkana designed a quick-release hand attachment device to deal with any physical safety-related events [10]. A new reflex mechanism structure based on an instinctive response behaviour pattern was adopted to ensure no harm or minimal harm to the user [9]. In ref. [11], a robotic task-practice system for the functional rehabilitation of arms was presented which maximized operational safety by designing a small overall workspace, not strapping the patent in and choosing only a-rotary-movement functional tasks. In order to improve security during functional recovery therapy, some therapy robots have been developed with pneumatic actuators [12, 13].

Generally, the role of the software is to monitor the distance between the user and the robotic arm, to check for dangerous proximity between the payload and other links to the robot, and to calculate the distance between the robot and nearby obstacles, which effectively prevents against collision [14]. Furthermore, some parameters (such as the force, torque and velocity) have limitations placed upon them to ensure control safety [3, 15, 16]. In ref. [17], a motion control method with an estimated danger index was proposed to monitor the user's safety and initiate proper safety actions in case of danger. In addition, impedance control has been extensively adopted to achieve compliance and security for human-machine interactions, creating a dynamic relationship between the force and position [18].

All the above-mentioned safety-based designs, whether with hardware or software, are effective to some extent, but the hardware-based methods are not online inherently and the software-based methods, having limited parameters, lack flexibility with regards to clinical application. However, most of the works are focused on collision prevention caused by exterior emergency factors, and few are concerned with sudden emergencies caused by interior factors, such as a spasm or twitch. Moreover, during rehabilitation exercises, many interior factors, such as pose or position changes and even coughing, usually cause some disturbance to the rehabilitation system. Thus, the designed control system should combine robustness and safety, and be able to effectively manage reasonable disturbances and sudden emergencies.

In this work, we investigate safety and robustness during rehabilitation exercises, assuming a training-impaired-limb is the object of the exercises. A real-time control system based on a safety supervisory strategy is designed, which mainly involves evaluating the physical state of the training impaired limb (PSTIL), a SSFC and a position-based impedance controller. The proposed SSFC makes decisions to adapt the desired force in response to reasonable disturbances, or to quickly stop the rehabilitation robot without doing harm to the training impaired limb when it suffers from a sudden spasm or twitch. Considering the essential characteristics of the PSTIL, the developed control system effectively combines robustness and safety and will perform a better rehabilitation exercise.

2. Feature Extraction

The upper-limb rehabilitation robot is a typical human-machine interaction system and usually the subject's affected limb comes into physical contact with the robotic end-effector in the course of the robot-aided movement treatments. During the robot-aided exercise, the training impaired-limb is not in an ideal static physical state, and there are many uncertain factors which affect the PSTIL, e.g., pose or position changes, sudden twitches, occasional tremors and even coughing or other external disturbances, which are partly subject to human control (another unresolved controller) [15]. Therefore, the PSTIL is dynamically variable, which influences the performance of the robotic control. It means that pose or position changes or sudden twitches made by the training impaired limb affect the performance of the position-velocity tracking. Thus, features of the position-velocity tracking errors represent the PSTIL to a certain extent.

The raw tracking error signals with noise are not directly used as input information to reflect the PSTIL. Therefore, certain features of the tracking errors are extracted in order to efficiently reflect the PSTIL. Among various extracted features, e.g., mean absolute value, average rectified value, mean absolute value slope, root mean square, mean square error (MSE), value range, and slope sign changes, MSE value is selected, in this paper, as a feature of tracking errors that can be extracted. The MSE value is widely used in applications for its good practicability and effectiveness in real-time control. The common MSE equation is expressed as the following:

$$\delta = \sqrt{\frac{1}{N-1}\sum_{i=1}^{N}(\bar{x} - x_i)^2} \tag{1}$$

where N is the number of sample data, $\bar{x}$ is the mean of the whole data, and x_i is the value of i^{th} sample data. In order to obtain the features more effectively and instantaneously for practical application, subsection sliding mean square error (SMSE) is adopted in this paper, which is expressed as

$$\begin{cases} \delta_k = \sqrt{\dfrac{1}{n-1}\sum_{i=1}^{n}(\bar{x}_k - x_{k-i})^2} \\ \bar{x}_k = \dfrac{1}{n}\sum_{i=1}^{n} x_{k-i} \end{cases} \tag{2}$$

where n is the number of sample data in the subsection, $\bar{x}_k$ denotes the mean of k^{th} subsection, x_{k-i} is the value of $(k-i)^{th}$ sample data, and δ_k is the corresponding feature of the k^{th} sample data.

3. Control System

3.1 Safety Supervisory Fuzzy Controller

Fuzzy control technology has been developed to achieve human-like comprehensive judgment. It is credited in various applications as a powerful tool providing robust approximation for systems [19]. Fuzzy control is well suited for rehabilitation robots for several reasons. Firstly, the rehabilitation-robot system is essentially nonlinear, which is difficult to accurately portray with a model. Focusing on a nonlinear system is an outstanding application for fuzzy control; therefore it is a reasonable control strategy for rehabilitation robots. Secondly, the rehabilitation robot is a real-time control system and must be managed using a quick-and-effective method of control. Fuzzy control well meets this requirement.

Safety and robustness are the primary principles in designing robot-aided neuro-rehabilitation control systems [20, 21]. We develop a SSFC to meet the requirements from the essential point of the PSTIL, which are of course essential to the mechanism. The designed SSFC consists of an input, fuzzy controller and a decision-making section, as per Fig. 1, which can automatically modify the desired force according to the PSTIL, or halt the robot in time if the user suffers from a sudden twitch.

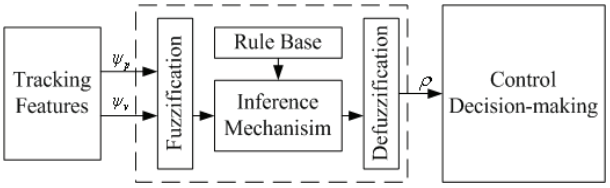

Figure 1. Structure of the SSFC

As mentioned above, the features of the position and velocity tracking errors are used to represent the PSTIL. Therefore, the fuzzy controller is adopted with two inputs and one output type. In order to achieve good performances under conditions of reasonable disturbances and emergencies, the inputs of the controller should include the information of the features and tracking-error variations. The used position and velocity information (ψ_p and ψ_v) are expressed as inputs as the following.

$$\begin{cases} \psi_p = f_{ep} + k_p \bullet f(e_{\max}, e_{\min}) \\ \psi_v = f_{ev} + k_v \bullet f(e_{\max}, e_{\min}) \end{cases} \tag{3}$$

where f_{ep} and f_{ev} are the features of the position and velocity tracking errors respectively, $f(e_{\max}, e_{\min})$ is a function to represent the tracking-error variation and k_p and k_v are ratios.

The corresponding output of the fuzzy controller is denoted by ρ which is related to the evaluated PSTIL. During the fuzzification and defuzzification, the inputs (ψ_p and ψ_v) and output (ρ) are scaled into five fuzzy sets, namely, negative zero (NZ), zero (ZE), positive small (PS), positive middle (PM) and positive big (PB), respectively. Triangle-shaped membership functions are selected for ZE, PS and PM, while trapezoidal membership functions are selected for NZ and PB. As mentioned above, the SSFC is developed with the aim of ensuring that the control system should be robust in case of reasonable disturbance and can avoid hurting the subject in an emergency situation. With robustness and safety in case of reasonable disturbance and emergency as their aim, the membership functions are designed with irregular shapes, as per Fig. 2, which can well serve the proposed control strategy according to the requirements of the PSTIL. Each combination of mapped inputs activates one control action according to the inference rule table (Table 1). Then, the value of ρ is obtained in the defuzzification process by using the centroid method:

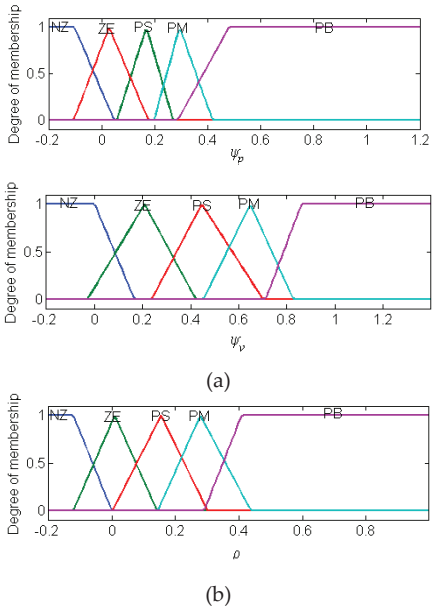

Figure 2. Input-output membership functions for SSFC. (a) Input membership functions; (b) Output membership functions

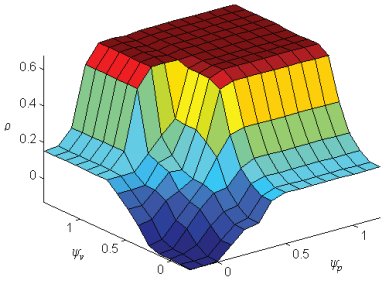

Figure 3. Control surface map for SSFC

ψ_v	ψ_p				
	NZ	ZE	PS	PM	PB
NZ	NZ	NZ	ZE	ZE	PS
ZE	NZ	ZE	PS	PS	PM
PS	ZE	PS	PS	PM	PB
PM	PS	PS	PM	PM	PB
PB	PS	PM	PB	PB	PB

Table 1. Fuzzy inference rules for output ρ

$$\rho = \frac{\sum_{i=1}^{n} \rho_i \cdot \mu_i}{\sum_{i=1}^{n} \mu_i} \tag{4}$$

where i indexes all the combinations of activated control actions from the rule table, ρ_i is the element in the physical universe of discourse of ρ, and u_i is the degree of membership of ρ_i. The overall control surface map of the intelligent supervisory controller is shown in Fig. 3. It clearly demonstrates that the output sharply increases in an emergency and the designed fuzzy controller manages the proposed strategy very well, differentiating between a reasonable disturbance and an emergency.

The decision-making section manages the rehabilitation training based on the evaluations of the PSTIL. In this research, in response to reasonable disturbance, the desired force is adapted with the following equation.

$$f_d(k) = f_d(k-1) + \rho f_e \tag{5}$$

where $f_d(k)$ and $f_d(k-1)$ are the corresponding desired forces between the end-effector and the impaired limb for k^{th} and $(k-1)^{th}$ intervals, respectively, and f_e is the actual interactive force between the robotic end-effector and the impaired limb.

Moreover, when the training impaired limb suffers from a sudden spasm or twitch, the emergency signal is given, which is shown as the following.

$$s = \begin{cases} 0 & \rho < \Gamma \\ 1 & \rho \geq \Gamma \end{cases} \tag{6}$$

where s is the emergency signal which denotes an emergency when it has a value of 1, otherwise it has a value of 0, and Γ is the threshold for an emergency.

3.2 Rehabilitation Robotic Control System

Upper-limb rehabilitation robots are used to assist those with neural injuries to help improve their motion function using rehabilitation trainings. One of the major difficulties in carrying out rehabilitation with robots is the controller design. The control system must be safe and robust enough, given the particular conditions of the subjects. As mentioned above, during robot-aided rehabilitation training, the PSTIL is dynamically variable. Therefore, suitable compliant behaviour between the robotic end-effector and the impaired limb is one of the primary requirements in designing the control system, especially with regards to the physical-contact rehabilitation robot. A well-established framework for managing this task is given by impedance control [22], which is an inherent model-based approach. According to the implement mode of target impedance, there are two general approaches, namely, position-based impedance control and torque-based impedance control [23]. In contrast to the torque-based control, the position-based control is more mature and the performance is more stable [18, 24]. Thus in this paper, the position-based impedance control is adopted to design the control system.

Impedance control achieves compliant motion by regulating the dynamic relationship between the robotic end-effector position/velocity and contact force. In this paper, the desired impedance equation of the rehabilitation robot can be represented by

$$\begin{cases} f_d = M_d \Delta\ddot{X} + B_d \Delta\dot{X} + K_d \Delta X \\ f_d = f(\rho, f_e) \end{cases} \tag{7}$$

$$\Delta X = X_d - X \,,\ \Delta\dot{X} = \dot{X}_d - \dot{X} \,,\ \Delta\ddot{X} = \ddot{X}_d - \ddot{X}$$

where M_d, B_d, K_d are desired inertia, damping and the stiffness matrix, respectively, X_d, X are the desired and actual position of the rehabilitation manipulator, $\dot{X}_d, \dot{X}$, $\ddot{X}_d, \ddot{X}$ are the corresponding velocities and accelerations. ρ and f_e are the output of the fuzzy controller and actual interactive force, respectively. In the frequency space, the equation (7) can be expressed as the following.

$$\frac{\Delta X(s)}{f_d(s)} = \frac{1}{M_d s^2 + B_d s + K_d} \tag{8}$$

During the rehabilitation exercise, the subject is part of the dynamic system and the PSTIL is also uncertain. Therefore, in this research, the control system of the rehabilitation robot is designed by incorporating the position-based impedance control and the proposed intelligent SSFC.

The overall control system block diagram is shown in Fig. 4, which mainly consists of an impedance controller, a position controller, the developed SSFC (including a feature generator, a fuzzy controller and decision-making response sections). The impedance controller brings about compliant behaviour between the robotic end-effector and the impaired limb and then the position controller is applied to execute the position tracking. In intelligent SSFC, the feature generator reflects the PSTIL in real time and the fuzzy controller supplies an output corresponding to the PSTIL to the response sections

which automatically adapt the desired force or halt the device using the so-designed decision-making mechanism. As analyzed above, the designed rehabilitation robotic control system is promises to be characterized by safety and robustness.

4. Experiments

4.1 Simulation Experiment

4.1.1 Simulation Model and setup

With regards to physical contact during the rehabilitation training, the complete dynamics [22, 25] of rigid serial n-link robot manipulator with n-degree-of-freedom revolute joints can be presented in the joint space as:

$$M(\theta)\ddot{\theta} + C(\theta,\dot{\theta})\dot{\theta} + G(\theta) = \tau - \tau_e \tag{9}$$

where $\theta, \dot{\theta}, \ddot{\theta} \in R^n$ represent position, velocity and acceleration of the rehabilitation robot in the joint space, respectively.

$M(\theta)$, $C(\theta,\dot{\theta}) \in R^{n\times n}$ represent symmetric positive-definite inertia matrix and the centripetal-Coriolis matrix, respectively.

$G(\theta) \in R^n$ represent gravitational terms.

τ, $\tau_e \in R^n$ represent the joint input torque vector and the generalized vector of joint torques exerted on the end-effector by the impaired limb, respectively.

The existing rehabilitation robot is usually designed with revolute joints to carry out the movement. In essence, the developed control algorithm manages the movement by controlling each joint rotation. Moreover, most of the trainings are executed with plane motions. Thus, in this research, in order to investigate the effectiveness of the proposed method, a two-link rehabilitation robot model (see Fig. 5) is used and several group simulation experiments were carried out on it.

The dynamics of the robot are given as:

$$M(\theta) = \begin{bmatrix} m_1 l_1^2 + m_2(l_1^2 + l_2^2 + 2l_1 l_2 \cos\theta_2) & m_2 l_2^2 + m_2 l_1 l_2 \cos\theta_2 \\ m_2 l_2^2 + m_2 l_1 l_2 \cos\theta_2 & m_2 l_2^2 \end{bmatrix},$$

$$C(\theta,\dot{\theta}) = \begin{bmatrix} -2m_2 l_1 l_2 \sin\theta_2 \dot{\theta}_2 & -m_2 l_1 l_2 \sin\theta_2 \dot{\theta}_2 \\ m_2 l_1 l_2 \sin\theta_2 \dot{\theta}_1 & 0 \end{bmatrix},$$

$$G(\theta) = \begin{bmatrix} m_2 l_2 g \sin(\theta_1 + \theta_2) + (m_1 + m_2) l_1 g \sin\theta_1 \\ m_2 l_2 g \sin(\theta_1 + \theta_2) \end{bmatrix}$$

In the simulation experiments, the parameters for the rehabilitation manipulator were selected as $l_1 = l_2 = 1m$, and $m_1 = 1.5kg, m_2 = 1.0kg$. The impedance control parameters (M_d, B_d, K_d) were chosen according to those in paper [22]. Parameter n in SMSE was set at 10 and the safety threshold Γ was selected as 0.6. The domains of the input-output variables in the proposed safety supervisory fuzzy algorithm were defined as $\psi_p \in [-0.2, 1.2]$, $\psi_v \in [-0.2, 1.4]$, $\rho \in [-0.2, 1.0]$.

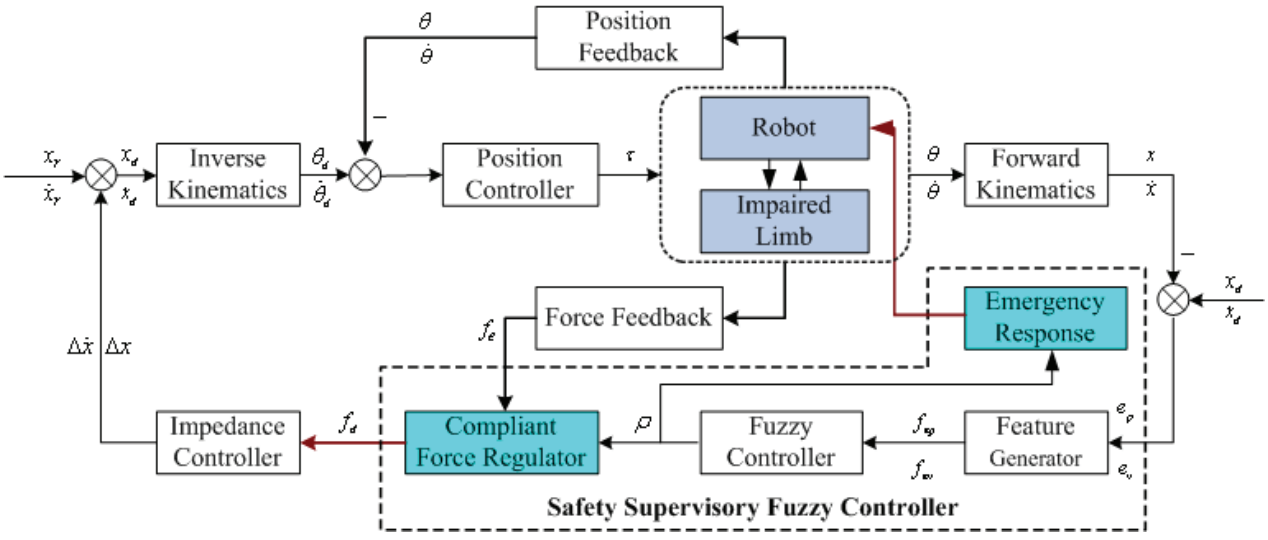

Figure 4. Control system block diagram for rehabilitation robot

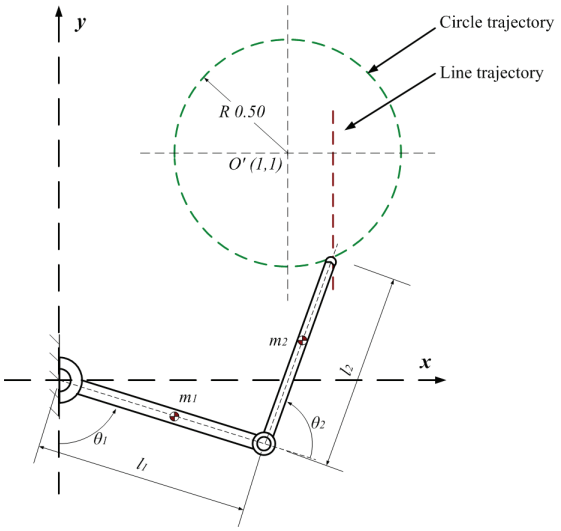

Figure 5. A two-link rehabilitation robot model

4.1.2 Predefined Trajectory and Simulated Signal

Reach and grasp skill training is critical for patients in their attempts to return to a reasonable quality of life [11, 26], because many daily living activities involve the use of the upper extremities [4, 27]. The linear reaching exercise [15, 28] is largely used at the early stages of rehabilitation, in order to reduce spasticity [8] and prevent contracture [29]. Circular movement is also commonly used in clinic robot-aided rehabilitation training [15, 18]. In this work, we designed the two typical movement trajectories, namely, linear and circular training trajectories.

The linear movement trajectory was predefined in the Y direction and the length was 0.8m with the starting position: (1.2, 0.4) and end position: (1.2, 1.2) and the cycle time was 16s (see Fig. 5). In Cartesian space, it is expressed as

$$\begin{cases} x = 1.2 \\ \begin{cases} y = 0.4 + 0.1t & t \le 8 \\ y = 2 - 0.1t & 8 < t \le 16 \end{cases} \end{cases} \tag{10}$$

The circular movement trajectory was predetermined with the centre point: (1, 1) and radius: 0.5m (see Fig. 5). In Cartesian space, it is expressed as

$$\begin{cases} x = 0.5\sin t + 1 \\ y = 0.5\sin(t + \dfrac{\pi}{2}) + 1 \end{cases} \tag{11}$$

To investigate the performance of the proposed method effectively, the planned movement ranges of predefined trajectories might be larger than those applied in clinics but this does not affect the analysis of control performances at all.

During rehabilitation exercises, the PSTIL generally presents three main types, these are 'rational state', the presence of reasonable disturbance and the occurrence of a sudden emergency. The interactive force is the only information shared between the impaired limb and robotic end-effector. Thus, in this research, interactive forces, corresponding to the different types of PSTIL, were used to investigate the control performances of the proposed strategy. Tremor is an involuntary, somewhat rhythmic, muscle contraction and relaxation involving to-and-fro movements (oscillations or twitching) of one or more body parts [30]. Neurological disorders or conditions (such as multiple sclerosis, stroke, traumatic brain injury and a number of neurodegenerative diseases that damage or destroy parts of the brainstem or the cerebellum) are liable to evoke tremors. Generally, the tremor is characterized by 3-to-8Hz oscillations or twitching [31]. Based on the characteristics of a tremor, we simulated interactive forces which are meant to represent a reasonable disturbance and a sudden emergency, respectively. In order to investigate the cases thoroughly, three kinds of interactive force, namely, regular sinusoid, sawtooth and complex sinusoid, were considered, which are shown in Table 2.

4.1.3 Feature Extraction Results

To demonstrate the performance of the feature extraction with SMSE, three kinds of experiments were carried out, namely, with S1, S2 and S3, respectively. In each experiment, the common interactive force between the end-effector and the impaired limb was set at 6N and the reasonable and emergency disturbances were applied during the sections 3~4s and 5~6s, respectively, of the total execution time of 10s. The experiments were carried out using a predefined circular trajectory and the simulated forces were exerted in X direction. The performances of feature extraction for position and velocity tracking errors in X direction were demonstrated in Fig. 6.

Signal type symbol	Reasonable disturbance	Emergency event (sudden twitch or spasm)
S1	$2\sin(10\pi t)$	$4\sin(10\pi t)$
S2	$4(5t-[5t])-2$	$8(5t-[5t])-4$
S3	$2\sin(8\pi t)+\sin(3\pi t)+rand()$	$6\sin(8\pi t)+3\sin(3\pi t)+rand()$

Table 2. Simulation Signals for the PSTIL

In Fig. 6, it can be clearly seen that the extracted features of position/velocity tracking errors in X direction during 3~4s, 5~6s and other sections are obviously different and the features under emergency (5~6s section) are remarkable, whether with S1, S2 or S3 disturbance. It indicates that the extracted features can represent the different PSTIL types, especially the emergency. From further analysis of Fig. 6, we see that the extracted features for different kinds of simulated states are consistent, which verifies the effectiveness of the proposed SMSE method for practical application. Comparing the feature during 3~4s with the one during 5~6s, the emergency can be detected easily. In other words, the extracted feature is only related to the upper-limb physical state to some extent.

4.1.4 Control Performance Results

As mentioned in section 3.2, impedance control has shown to be promising in achieving compliant behaviour; therefore many researchers have adopted and developed this method for their control strategies. In this paper, in order to ensure robustness and safety, a method has been suggested which develops the intelligent SSFC (see Fig. 4) by combining it with the traditional position-based impedance control [8, 24, 32]. To investigate the control performances of the two methods, namely, the proposed method and traditional position-based impedance control, diverse experiments were planned. The simulations were carried out with predefined linear and circular trajectories, respectively, and two formal simulated signals (S1 and S3) were selected to test the control performance for each trajectory movement in order to verify the universal effectiveness of the proposed method. During the movement of the circular trajectory, the method of exerting the simulated disturbances of the different PSTIL was the same as mentioned in section 4.1.3. During the movement of the linear trajectory, the simulated disturbances were exerted in Y direction. The overall comparison of the control performances of linear movement is shown in Figs. 7 and 8, for S1 and S3, respectively. By comparing the velocity-tracking performances in Y direction between the proposed and traditional position-based impedance control, it is evident in Fig. 7(b) and 8(b) that, at the beginning, the proposed strategy presents a preferable initial response. Meanwhile, the proposed method presents a better position tracking performance than the traditional method, which is demonstrated in Fig. 7(d) and 8(d). Furthermore, it can effectively detect an emergency in real time, which represents a notable advantage with respect to safety. Emergency signals are supplied at 5.02s and 5.19s according to the evaluated PSTIL, as shown in Figs. 7(a) and 8(a), respectively, which correspond to the imitative impaired-limb condition.

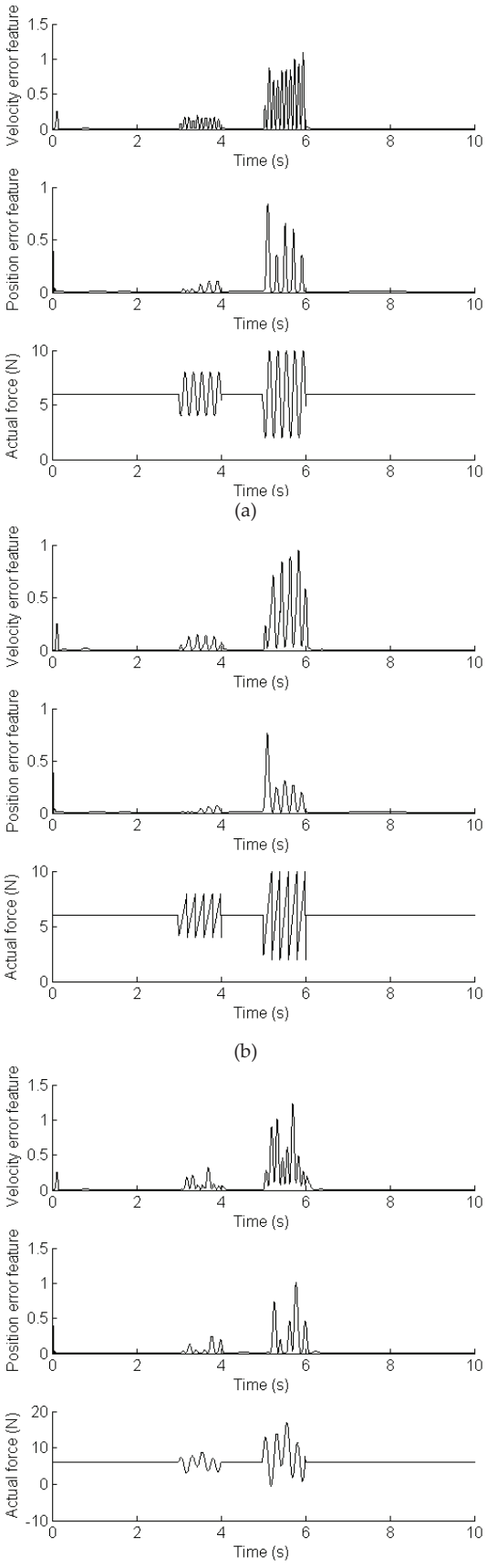

Figure 6. Feature extraction under different kinds of disturbances. (a) S1; (b) S2; (c) S3

Figs. 9 and 10 show the compared control performances for circular movement, for S1 and S3, respectively. The velocity tracking errors in X direction for S1 and S3 are shown in Fig. 9(b) and 10(b). The same conclusion is drawn as previously: that the suggested strategy presents a better initial response than the traditional method. Figs. 9(a) and 10(a) show the detecting performances of the proposed method and the emergency was detected at 5.01s and 5.17s for S1 and S3, respectively. The end-effector tracking performances in Fig. 9(d) and 10(d) reveal that the proposed strategy also provides better position tracking capability for circular movement.

To come to an overall appraisal of the proposed and traditional methods, the results were further analyzed with three indices, namely, overshoot (the maximum absolute error during the adjusting procedure), the sum of the absolute error (SAE) and maximum deviation (MD, the maximum absolute error during the 3~5s). Here, the recording data from 0~5s was selected to investigate the performance because the proposed strategy halted the robot in real time due to a simulated emergency. Two cases (position and velocity tracking errors) were studied to demonstrate the control performances. The analyses of the results of control performances are shown in Tables 3 and 4, for S1 and S3, respectively. According to the results, the method proposed with smaller overshoot provides better stability than the traditional method. Meanwhile, the results indicate that the novel control system with proposed method outperforms the traditional control system on trajectory tracking. Most importantly, the proposed method can effectively detect emergencies and works more safely and robustly.

Trajectory type	Method	Position tracking error (m)			Velocity tracking error (m/s)		
		Overshoot	SAE	MD	Overshoot	SAE	MD
Linear	Traditional	0.022493	89.54	0.014475	0.069707	14.085	0.00089361
	Proposed	0.021236	87.323	0.013226	0.049541	8.6949	0.00028771
Circular	Traditional	0.045553	101.89	0.029501	0.7652	224.57	0.054908
	Proposed	0.022774	50.169	0.013501	0.61179	139.61	0.033607

Table 3. Control performance comparisons for S1. During the circular movement, the position tracking error is defined along the radial direction and the analyzed velocity is in X direction. The sample frequency is set at 1kHz.

Trajectory type	Method	Position tracking error (m)			Velocity tracking error (m/s)		
		Overshoot	SAE	MD	Overshoot	SAE	MD
Linear	Traditional	0.022491	88.579	0.012183	0.069707	14.438	0.0015265
	Proposed	0.021236	86.367	0.011072	0.049541	8.7986	0.00041349
Circular	Traditional	0.045553	97.459	0.022614	0.76521	245.6	0.092167
	Proposed	0.022773	46.66	0.011087	0.61179	154.25	0.048954

Table 4. Control performance comparisons for S3. During the circular movement, the position tracking error is defined along the radial direction and the analyzed velocity is in X direction. The sample frequency is set at 1kHz.

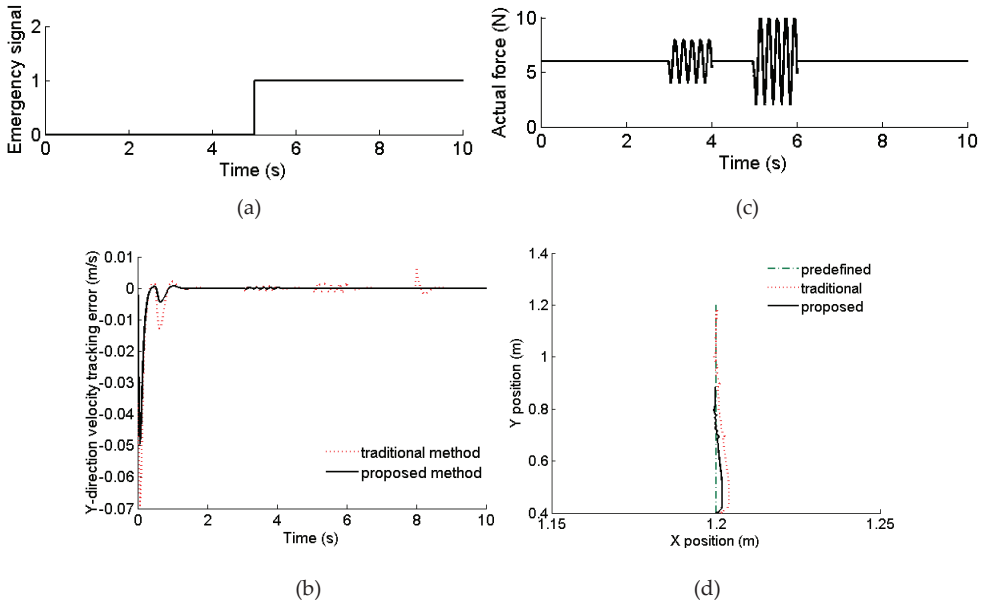

Figure 7. Control performances of linear movement and emergency detection: S1. (a) Emergency signal; (b) Velocity tracking comparison; (c) Actual force with S1; (d) Trajectory tracking comparison

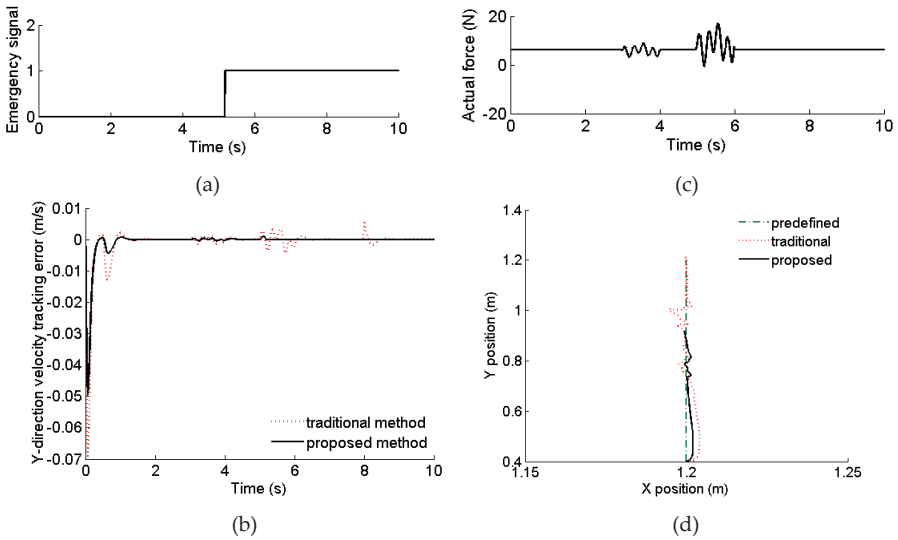

Figure 8. Control performances of linear movement and emergency detection: S3. (a) Emergency signal; (b) Velocity tracking comparison; (c) Actual force with S3; (d) Trajectory tracking comparison

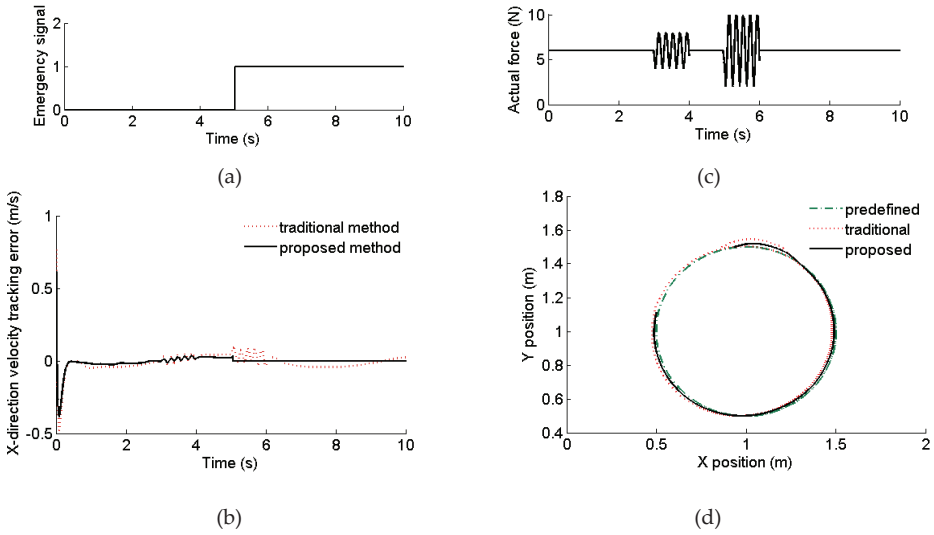

Figure 9. Control performances of circular movement and emergency detection: S1. (a) Emergency signal; (b) Velocity tracking comparison; (c) Actual force with S1; (d) Trajectory tracking comparison

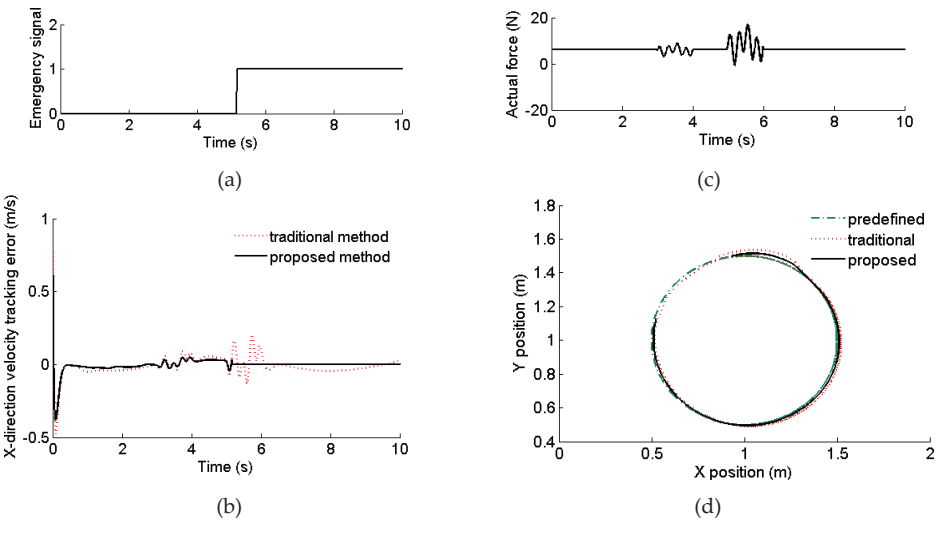

Figure 10. Control performances of circular movement and emergency detection: S3. (a) Emergency signal; (b) Velocity tracking comparison; (c) Actual force with S3; (d) Trajectory tracking comparison

4.2 Real Experiment

4.2.1 Experiment setup

Additionally, the proposed control strategy was further verified on a WAM rehabilitation robot. The WAM rehabilitation system mainly consists of the Barrett WAM Arm, a 3-D force sensor [33], an arm supported device, and an external PC, as shown in Fig .11. The standard WAM Arm is a four degree-of-freedom (DOF) highly dexterous, naturally back-drivable manipulator, which stretches the impaired limb for movement exercises. The improved 3-D force sensor was designed and installed on the end-effector to record the interactive force during the exercises and the arm supported device was designed to support the forearm of the stroke participant. The proposed control strategy was developed on an external PC with Ubuntu Linux system. More detailed information on WAM rehabilitation systems is given in ref. [20].

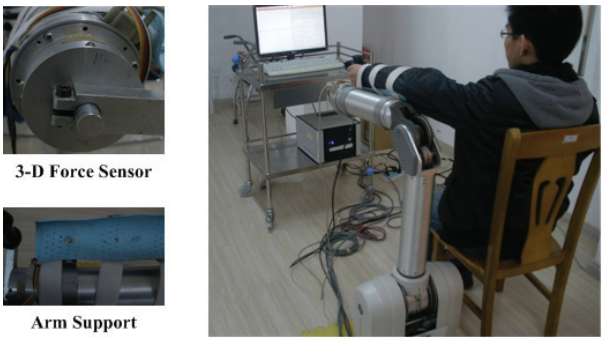

Figure 11. WAM rehabilitation system

4.2.2 Experiment scheme

A shoulder extension/flexion, horizontal movement trajectory was predefined, whose range, expressed in the WAM Arm's world coordinates, was defined as 0.45 rad in flexion and −0.45 rad in extension (XOY plane), with 18.1s for each session. A healthy adult male volunteer was instructed to deliberately simulate the different PSTIL during the rehabilitation exercise. The volunteer was required to simulate each type of physical state (reasonable disturbance and sudden twitch) as much as possible with the same action and at the same position. In order to avoid unfairly influencing the experiment results, the volunteer was firstly asked to do extensive simulating exercises, moreover, each experiment was carried out five times. The eventual outcome was derived from the average of the 5 results.

4.2.3 Control Performance

To demonstrate the superiority of the proposed strategy, the proposed and traditional control methods were used on the WAM rehabilitation system, respectively. The position and velocity tracking errors were recorded during the experimental exercise and at the same time the emergency signal was also recorded when the rehabilitation system was running with the proposed method. The experimental results are shown in Fig.12. The subject simulated reasonable disturbance and emergency at 8~10s and 26.5~28.5s, respectively.

In Fig.12, comparing the position and velocity tracking errors of two control methods, it can be concluded that the proposed method presents a better tracking performance, which is strikingly similar to the result of simulation experiments. The proposed method supplied an emergency signal to halt the rehabilitation exercise at 27.48s when the impaired limb was suffering from an emergency, which demonstrates remarkable superiority with regards to safety. The data from the first exercise session was further analyzed to present the control performances of the proposed and traditional methods. Note that the data of the second session is exclusive, because the proposed method halted the rehabilitation exercise due to an emergency to protect the impaired limb. Two indices, the maximum of the absolute error (MAE) and the sum of absolute error (SAE) of the trajectory tracking errors, were adopted to evaluate position and velocity tracking performances of two controllers. The outcomes are presented in Table 5. The analyzed results also show that the proposed method runs rehabilitation training with a better tracking performance than the traditional method in the presence of reasonable disturbance.

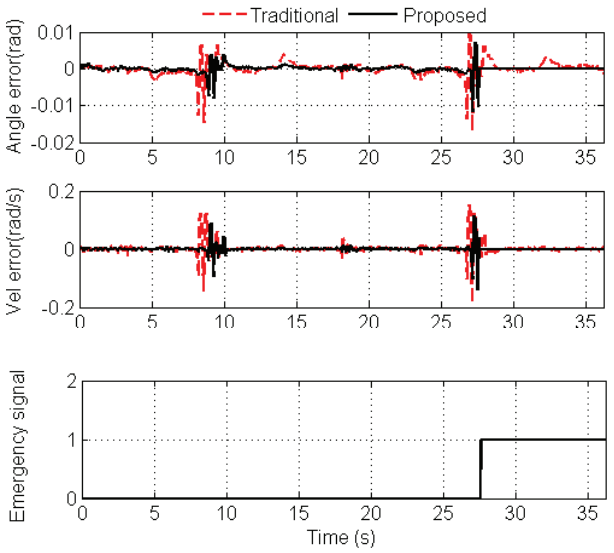

Figure 12. Control Performance comparison

Control performances		Methods	
		Proposed	Traditional
Position tracking (rad)	MAE	0.007872	0.014617
	SAE	0.98999	2.0945
Velocity tracking (rad/s)	MAE	0.094944	0.14499
	SAE	6.9344	13.278

Table 5. Control performance comparison of proposed and traditional methods

5. Conclusions

System security and the robustness of the controller are the critical considerations when designing a rehabilitation robot. In this paper, we present a novel safety supervisory control strategy to meet the demands that the system be robust when faced with reasonable disturbance and safe enough in emergencies. The proposed method is highly suitable for the real-time safety monitor. Regarding the training impaired limb itself, the features of the position and velocity tracking errors were extracted to evaluate the physical state of the limb in real time. A safety supervisory fuzzy controller was developed to achieve systematic safety and robustness. The fuzzy controller automatically adapts the desired force between the end-effector and impaired limb to ensure robustness in the event of reasonable disturbance. Furthermore, the fuzzy controller can effectively detect an emergency such as a sudden spasm or twitch etc, and halt the robot quickly enough so as to avoid causing the impaired limb further harm during the emergency. Meanwhile, a position-based impedance controller has been designed to achieve interactive compliance during the rehabilitation trainings. The diverse simulation and real experimental results have verified the effectiveness and practicability of the proposed method to achieve security and robustness for an upper-limb rehabilitation robot.

6. Acknowledgements

The authors appreciate the help of all their colleagues in the Remote Measuring and Control Laboratory, who made valuable contributions to this work. This work was supported by the National Natural Science Foundation of China (No. 61104206, No. 61105048, No. 61272379), the Natural Science Foundation of JiangSu Province (BK2010063), the Technology Project Foundation of JiangSu Province (BE2012740), the Industrial Technology Project Foundation of the ChangZhou Government (CE20120085), and the Ph.D. Program Foundation of the Ministry of Education of China (No. 20110092120034). The authors would also like to thank the anonymous reviewers for their very useful comments.

7. References

[1] American Heart Association: Heart and Stroke Statistical Update (2011). Available: http://www.Americanheart.org/statistics/stroke.htm.

[2] B.G. Xu, S. Peng, A.G. Song, "Robot-Aided Upper-Limb Rehabilitation Based on Motor Imagery EEG," *Int J Adv Robotic Sy*, vol. 8, no. 4, pp. 88-97, 2011.

[3] P.R. Culmer, A.E. Jackson, S. Makower, "A Control Strategy for Upper Limb Robotic Rehabilitation With a Dual Robot System," *IEEE/ASME Transactions on Mechatronics*, vol. 15, no. 4, pp. 575-585, 2010 .

[4] K. Kiguchi, M.H. Rahman, M. Sasaki, K. Teramoto, "Development of a 3DOF mobile exoskeleton robot for human upper-limb motion assist," *Robotics and Autonomous Systems*, vol. 58, pp. 678-691, 2008.

[5] D.J. Reinkensmeyer, J.L. Emken, S.C. Cramer, "How to retrain movement after neurologic injury: a computational rationale for incorporating robot (or therapist) assistance," *Proceedings of the 25th Annual International Conference of the IEEE*, pp. 1479-1482, 2003.

[6] R. Riener, T. Nef, G. Colombo, "Robot-aided neurorehabilitation of the upper extremities," *Med Biol Eng Comput*, vol. 43, no. 1, pp. 2-10, 2005.

[7] P.S. Lum, G. Uswatte, E. Taub, "A telerehabilitation approach to delivery of constraint-induced movement therapy," *Rehabil Res*, vol. 43, no. 3, pp. 391-400, 2006.

[8] M.C. Laura, J. David, "Review of control strategies for robotic movement training after neurologic injury," *Journal of Neuro Engineering and Rehabilitation*, 6:20, 2009.

[9] N. Tejima, D. Stefanov, "Fail-Safe Components for Rehabilitation Robots-A Reflex Mechanism and Fail-Safe Force Sensor," *Proceedings of the 9th International Conference on Rehabilitation Robotics*, Chicago, USA, 2005.

[10] D. Barkana, J. Das, F. Wang, "Incorporating verbal feedback into a robot-assisted rehabilitation system," *Robotica*, vol. 29, no. 3, pp. 433–443, 2011.

[11] C. Younggeun, J. Gordon, K. Duckho, "An Adaptive Automated Robotic Task-Practice System for Rehabilitation of Arm Functions After Stroke," *IEEE Transactions on Robotics*, vol. 25, no. 3, pp. 556-568, 2009.

[12] R. Morales, J.B. Francisco, G.A. Nicolás, "Pneumatic robotic systems for upper limb rehabilitation," *Med Biol Eng Comput*, vol. 49, no. 10, pp. 1145-1156, 2011.

[13] K. Kirihara, N. Saga, N. Saito, "Design and control of an upper limb rehabilitation support device for disabled people using a pneumatic cylinder" *Industrial Robot an International*, vol. 37, no. 4, pp. 354-363, 2010.

[14] F. Fusco, R. Gallerini, "Robotic Arm: the Problem of Preventing Collisions" *The 6th ESA Workshop on Advanced Space Technologies for Robotics and Automation*, ESTEC, Noordwijk, 2000.

[15] M.S. Ju, C.C.K. Lin, D.H. Lin, Ing-Shiou Hwang, "A Rehabilitation Robot with Force-Position Hybrid Fuzzy Controller: Hybrid Fuzzy Control of Rehabilitation Robot," *IEEE Transactions on Neural Systems and Rehabilitation Engineering*, vol. 13, no. 3, pp. 349-358, 2005.

[16] N. Tejima, K. Araki, "Rehabilitation robot risk reduction by three-dimensional force limitation and reflex mechanism," *Proceedings of the ICORR*, 2003.

[17] P. Aslam, R. Jeha, "Safe physical human–robot interaction of mobility assistance robots: evaluation index and control," *Robotica*, vol. 29, pp. 767–785, 2011.

[18] H.I. Krebs, B.T. Volpe, N. Hogan, "Robotic applications in neuromotor rehabilitation," *Robotica*, vol. 21, no. 3, pp. 3-11, 2003.
[19] H. Chaoui, P. Sicard, "Adaptive Fuzzy Logic Control of Permanent Magnet Synchronous Machines With Nonlinear Friction," *IEEE Transactions on Industrial Electronics*, vol. 59, no. 2, pp. 1123-1133, 2012.
[20] G.Z. Xu, A.G. Song, H.J. Li, "Control System Design for an Upper-Limb Rehabilitation Robot," *Advanced Robotics*, vol.25, pp. 229–251, 2011.
[21] P. Beyl, K. Knaepen, S. Duerinck, "Safe and Compliant Guidance by a Powered Knee Exoskeleton for Robot-Assisted Rehabilitation of Gait," *Advanced Robotics*, vol. 25, no. 5, pp. 513-535, 2011.
[22] N. Hogan, "Impedance Control: An approach to manipulation: Part 1-theory, Part 2-Implementation, and Part 3-Application," *ASME J. of Dynamic Systems, Measurement and Control*, vol.107, pp. 1-24, 1985.
[23] D. Lawrence, M.M. Denver, "Impedance control stability properties in common implementations," *IEEE Int Conf on Robot and Auto,* vol. 2, pp. 1185-1190, 1988.
[24] Y. Yang, L. Wang, L.X. Zhang, "Arm Rehabilitation Robot Impedance Control and Experimentation," *in Proceedings of the ROBIO*, 2006.
[25] H.S. Liu, K.R. Hao, X.B. Lai, "Fuzzy Saturated Output Feedback Tracking Control for Robot Manipulators: A Singular Perturbation Theory Based Approach," *Int J Adv Robotic Sy,* vol. 8, no. 4, pp. 43-53, 2011.
[26] J.H. Carr, R.B. Shepherd, "Stroke Rehabilitation Guidelines for Exercise and Training to Optimize Motor Skill," London, U.K.: Butter-worth/Heinemann, 2003.
[27] W.J. Coster, S.M. Haley, P.L. Andres, "Refining the conceptual basis for rehabilitation outcome measurement: Personal care and instrumental activities domain," *Med. Care*, vol. 42, pp. 162-172, 2004.
[28] L.E Kahn, M.L Zygman, W.Z. Rymer, "Robot-assisted reaching exercise promotes arm movement recovery in chronic hemiparetic stroke: a randomized controlled pilot study," *Journal of NeuroEngineering and Rehabilitation*, vol. 3, no.12, 2006.
[29] P.E. Williams, "Use of intermittent stretch in the prevention of serial sarcomere loss in immobilised muscle," *Ann Rheum Dis*, vol. 49, no.5, pp. 316-317, 1990.
[30] G. Cooper, R. Rodnitzky, "The many forms of tremor: Precise classification guides selection of therapy," *Postgrad Med,* vol. 108, 2000.
[31] B. Hellwig, P. Mund, "A longitudinal study of tremor frequencies in Parkinson's disease and essential tremor," *Clinical Neurophysiology*, vol. 120, no. 2, pp. 431-435, 2009.
[32] S. Hussain, S.Q. Xie, G.Y. Liu, "Robot assisted treadmill training: Mechanisms and training strategies," *Med Eng and Phys*, vol. 33, no. 5, pp. 527-533, 2011.
[33] A.G. Song, J. Wu, G. Qin, W.Y. Huang, "A novel self-decoupled four degree-of-freedom wrist force/torque sensor," *Measurement*, vol. 40, no. 9, pp. 883-889, 2007.